

---

## Cellular automata model for stock market dynamics

In the previous chapter we analyzed different sets of empirical data from financial markets in order to shed some light on the dynamics of this complex system. In particular, we investigated the underlying self-organization processes, whose manifestations, such as power laws and log-periodic oscillations, can be related to *self-organized criticality* and *discrete scale invariance*, respectively.

In the present chapter we use a different approach. We try to understand the microscopic trading dynamics between the agents by actually simulating it and, afterwards, testing the results against real data. In our model we emphasize, in particular, the herding behaviour of the agents which live in an *open* market. That is, their number, as well as their information network, changes in time. The clustering among the agents is reproduced via a stochastic cellular automata (CA). CA, which we already mentioned in the introduction of this thesis as a paradigm for complexity, are discrete dynamical systems in both space and time: the elementary parts are cells arranged on a regular grid which interact with their neighbours at each time step. The variables characterizing the state of each cell are also discrete. The use of CA leads to a quite significant advantage when dealing with non-linear extended systems. Whereas, the use of a continuous models (such as sets of differential equations) is subject to non negligible numerical errors, with CA the emergent behaviour of the system is simulated just by the application of local rules between the cells. In this case there are no numerical round-off. For a detailed discussion on the subject, that goes beyond the scope of this chapter, see Ref. [Wol86].

In the CA model, introduced in detail in Sec. 3.2, the rules are related to a *direct percolation* phenomenon and they are used to generate a hierarchy of clusters of active traders on a two dimensional grid. Active traders are characterized by the decision to buy,  $\sigma_i(t) = +1$ , or sell,  $\sigma_i(t) = -1$ , a stock at a certain discrete time step. The remaining cells are inactive,  $\sigma_i(t) = 0$ . The trading dynamics, that is the spin orientation, is then determined by the stochastic interaction between traders belonging to the same cluster. Extreme, intermittent events, like crashes, are triggered by a phase transition in the state of the bigger clusters present on the grid, where almost all the active traders come to share the same

spin orientation. Price fluctuations obtained with the model are then tested against the daily closures of the S&P500 index for the US market in Sec. 3.3. Most of the stylized facts of the time series summarized in Sec. 3.1, and the multifractal properties, summarized in Sec. 3.4, are reproduced by the model. The present chapter is based on a previously published work, Ref. [BT04].

### 3.1 Basic stylized facts of the stock market dynamics: a brief overview

Since the successful application of the Black-Scholes theory for option pricing [BS73, MB73] in 1973 more and more physicists have been attracted by the idea of understanding the behaviour of market dynamics in terms of complex system theory, where self-organized criticality [BTW87, Bak99, Jen98, BPS97] and stochastic processes [MS99, PB99, BP99] play important roles. The aim of the microscopic models proposed so far (for general reviews [LLS00, Fei03]) is to reproduce some *stylized facts* [SST99] concerning the temporal fluctuations of the price indices,  $P_r(t)$ , that we already considered in the previous chapter. In particular, the *logarithmic price returns*, Eq. (2.1), and the *volatility*, Eq. (2.7), have been studied extensively [MS99, BP99] from an empirical point of view. The results have shown that while long time correlations are present in the volatility, a phenomenon known as *volatility clustering*, they cannot be found in the time series of returns. Moreover the latter show an intermittent behaviour resembling hydrodynamic turbulence [MS97, MS95, Fri95], characterized by power law tails in the probability distribution function (PDF),  $P$ . Microsimulations have demonstrated that this kind of behaviour can originate both as a stochastic process with multiplicative noise [Kai00, KHH02, TST97, TT99] and as a percolation phenomenon [Sta85, SP98, CB00].

In order to reproduce these features of real markets we introduce a stochastic cellular automata model, representing an *open* market. That is, a market where the number of *active* traders, defined as cells with spin state different from 0, namely  $\sigma_i(t) = \pm 1$ , evolve in time according to a percolation dynamics. The percolation dynamics is chosen in order to simulate the herding behaviour typical of investors [SZ03]. According to this, active traders gather in *clusters* or *networks* where, following a stochastic exchange of information, they formulate the trading strategy for the next time step. The results obtained by the simulations are then compared with the time series of daily closures of the S&P500 index [MS99, Pea99, CLM<sup>+</sup>97, GPA<sup>+</sup>97, Lea99, SZ03, AI03, TABO03, Can00] over a period of about 50 years in Sec. 3.3.

Moreover, the fractal properties [Fed88] of price fluctuations have been investigated recently for different markets [RNZR<sup>+</sup>01, GDS02, AI02, DMAD03]. A common feature found in these studies is the existence of a nonlinear, multifractal spectrum that excludes the possibility of *efficient market* behaviour [Bac00]. The origin of multifractality of in the financial time series has also been at the center of discussions [Lux01, Man01, LeB01, SP01]. In this context we simply consider the multifractal spectrum of the price fluctuations as a further stylized fact of the market time series without addressing any question about the underlying process able to generate it. The multifractal spectrum is used as a further test for our model. These results are presented in Sec. 3.4. In the same section, a parallel between the multifractal and thermodynamical formalisms is investigated. We find, in agreement with the previous work of Canessa [Can00], that the *analogue specific heat*,  $C_q$ , can provide a good tool to characterize intermittency, that is financial crashes or bubbles, from a thermodynamic-equivalent point of view.

## 3.2 The cellular automata model

The financial market dynamics is simulated via a stochastic cellular automata. The agents of the market are represented by cells on a two dimensional grid, 512x128. The  $i$ th agent at the discrete time step  $t$  is characterized by three possible states or spin orientations,  $\sigma_i(t) = 0, \pm 1$ . The value  $\sigma_i(t) = +1$  is associated with the purchase of a stock while  $\sigma_i(t) = -1$  with selling. The former states are called *active*. The cells with spin value  $\sigma_i(t) = 0$  are *inactive* traders. The active traders herd in *networks* or *clusters* via a direct percolation method related to a *forest fire* model [Jen98]. The information carried by the active traders, that is their spin state, is shared with the other members of the cluster. The percolation dynamics allow a time dependent herding behaviour and the market can be interpreted as an open system not bounded by conservation laws. The clustering process will be discussed in detail in the next subsection.

The trading dynamics is instead related to the synchronous update of the spins of the active traders, ruled by a stochastic exchange of information between them, similar to a random Ising model [Kai00, KHH02]. A particular feature of the present simulation is that the information is not spread all over the grid, as in other multi-agent scenarios [Kai00, KHH02], but it is limited by the clusters of interaction previously defined. The mechanism for the spin dynamics is explained in subsection 3.2.2.

### 3.2.1 Percolation clustering

One of the aims of our cellular automata model is to reproduce the *herding behaviour* of active traders [SZ03]. We refer to herding behaviour as the tendency of people involved in the market to aggregate in networks or clusters of influence. The traders then use the information obtained by their network in order to formulate a market strategy. Even if the topological structure of these networks of information can be neglected as a first approximation, since several kinds of long range interaction are available nowadays [KHH02], the number of connections for each trader must be, in any case, finite and not extended over the whole market. In this framework a direct percolation method is used to simulate herding dynamics between active traders where the definition of the neighbours is the one of von Neumann (up, down, left, right). The *synchronous* updating is fixed by the following parameters:

$p_h$ : the probability that an active trader can turn one of his inactive neighbours into an active one at the next time step,  $\sigma_i(t) = 0 \rightarrow \sigma_i(t+1) = \pm 1$ . This simulates the fact that certain information possessed by a trader may induce a *potential* trader to join the market dynamics.

$p_d$ : the probability, for *each* of its inactive neighbours, that an active trader *diffuses* and so becomes inactive,  $\sigma_i(t) = \pm 1 \rightarrow \sigma_i(t+1) = 0$ . This mimics the fact that only traders at the borders of a network, that is the weaker links, can quit the market.

$p_e$ : the probability that a non trading cell spontaneously decides to enter the market dynamics,  $\sigma_i(t) = 0 \rightarrow \sigma_i(t+1) = \pm 1$ .

The values of the adimensional parameters,  $p_h$ ,  $p_d$  and  $p_e$ , influence the stability of the system and the percentage of active traders on the grid. In order to test different market activities we fix the values  $p_d = 0.05$  and  $p_e = 0.0001$  while we tune the parameter  $p_h$ . At the beginning of the simulation the grid is loaded randomly with a small percentage of active traders and then the system is permitted to evolve according to the previous rules. If we are in a stable range of the parameter  $p_h$ , after a transient period that depends both on the parameter values and the initial number of active cells, the total number of active traders on the grid begins to fluctuate around a certain average, as shown in Fig. 3.1 (Top). The market can be considered *open* since the number of agents changes dynamically in time. In this regime, the competition between herding and diffusion produces a power law distribution of the cluster size, as shown in Fig.3.1 (Bottom),  $\rho(S) \approx S^{-\lambda}$ , where  $S$  is the cluster dimension, defined as the number of active cells belonging to the same cluster, and  $\lambda > 0$ , creating a hierarchy of networks. This hierarchy is necessary if we are to take into account a real aspect of the market, namely that different traders also have different

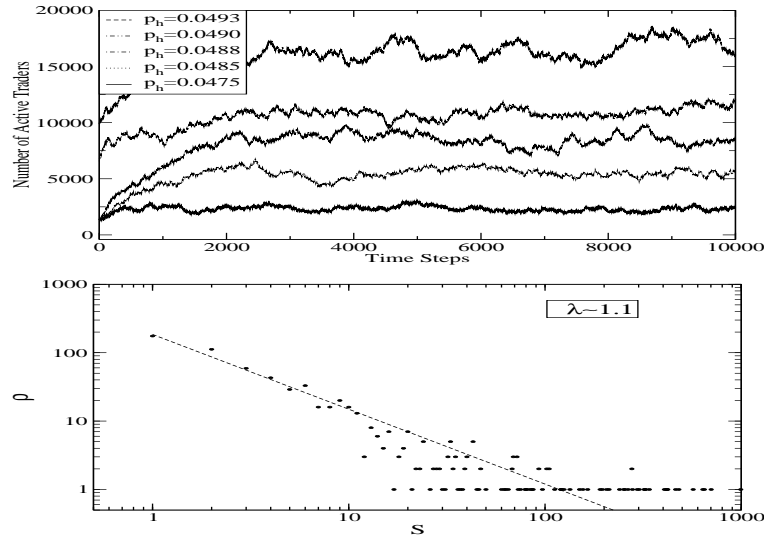


Figure 3.1: Top: Different values of the parameter  $p_h$  produce different activities of traders on the grid. Bottom: Cluster size distribution for  $p_h = 0.0485$  at  $t = 9000$ .

trading powers. A reasonable assumption is that people having a larger number of sources of information, so belonging to greater clusters, can be associated with professional investors that, most likely, are able to move a greater amount of stocks compared to the occasional investor. Using this assumption we are able to define a proper weight for the trading power of different cells, as we will discuss in the next subsection.

A similar percolation model has also been used to reproduce some statistical and geometrical features of solar activity [WS92, WS96, VFHG02].

### 3.2.2 Stochastic trading dynamics

The dynamics of the spins of the active traders,  $\sigma_i^k(t) = \pm 1$  for  $i = 1, \dots, N^k(t)$  (where the superscript  $k$ , from now on, refers to the  $k$ th cluster of the grid configuration at time step  $t$ ) follows a stochastic process that mimics the human uncertainty in decision making [KHH02]. Their values are updated synchronously according to a local probabilistic rule:  $\sigma_i^k(t+1) = +1$  with probability  $p_i^k$  and  $\sigma_i^k(t+1) = -1$  with probability  $1 - p_i^k$ . The probability  $p_i^k$  is determined, by analogy to heat bath dynamics with formal temperature  $k_B T = 1$ , with  $k_B$  the

Boltzmann constant, by

$$p_i^k(t) = \frac{1}{1 + e^{-2I_i^k(t)}}, \quad (3.1)$$

where the local field,  $I_i^k(t)$ , is

$$I_i^k(t) = \frac{1}{N^k(t)} \sum_{j=1}^{N^k(t)} A_{ij}^k \sigma_j^k(t) + h_i^k. \quad (3.2)$$

The  $A_{ij}^k(t)$  are time dependent interaction strengths between agents and  $h_i^k(t)$  is an external field reflecting the effect of the environment [KHH02]. The interaction strengths and the external field change randomly in time according to  $A_{ij}^k(t) = A\xi^k(t) + a\eta_{ij}(t)$  and  $h_i^k(t) = h\zeta_i^k(t)$ . The variables  $\xi^k(t)$ ,  $\eta_{ij}(t)$ ,  $\zeta_i^k(t)$  are random variables uniformly distributed in the interval (-1,1) with no correlation in time or space. The measure of the strengths of the previous terms,  $A$ ,  $a$  and  $h$ , are constant and common for all the grid.

In this context the dynamics of the price index,  $P_r(t)$ , can be easily derived if we assume that the index variation is proportional to the difference between demand and supply,

$$\frac{dP_r}{dt} \propto xP_r, \quad (3.3)$$

and using a weighted average for the orientation of the spins,

$$x(t) = \beta \sum_{k=1}^{N_{cl}(t)} \sum_{i=1}^{N^k(t)} N^k(t) \sigma_i^k(t), \quad (3.4)$$

where  $N_{cl}(t)$  and  $N^k(t)$  are, respectively, the number of clusters on the grid and the size of the  $k$ th cluster, while  $\beta$  is a normalization constant. The relation (3.4) follows from the assumption of proportionality between the financial power of an active cell and the size of the cluster to which it belongs. A justification of this relation is that professional investors, able to move larger amounts of capital, are more likely to be linked with a large number of other investors than the occasional traders. From (3.3) we find that the logarithm of the price returns, Eq. (2.1), that is the fundamental quantity we aim to model, is proportional to the average orientation defined in Eq. (3.4),  $r(t) \propto x(t)$ .

### 3.3 Numerical results and comparison with the S&P500

We compare the results of our model with the Standard & Poor 500 (S&P500) index that is one of the most widely used benchmarks for US equity perfor-

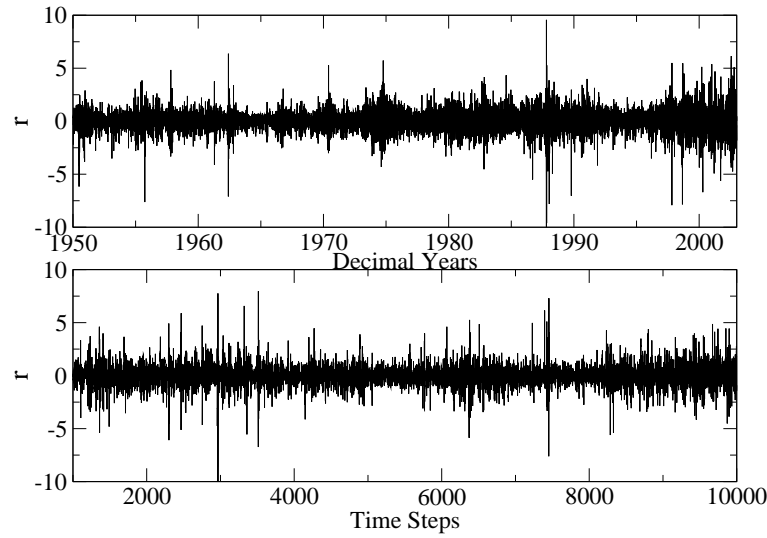


Figure 3.2: Top: Normalized logarithmic returns for the S&P500. Bottom: Time series of returns reproduced with the simulation with  $p_h = 0.0493$ ,  $A = 1.8$  and  $h = 0$ .

mance. The database analyzed is composed of the daily indices from 3/1/1950 to 18/7/2003 for a total of 13468 data. The time series of the index prices,  $P_r(t)$ , is converted into the logarithmic returns, Eq. (2.1), and then normalized over the time interval under consideration according to Eq. (2.2). In this way all the sets of returns will have zero average and  $\sigma = 1$ .

Before discussing the results we briefly describe the behaviour of the cellular automata with respect to changes of the parameters. Regarding the percolation, the herding parameter  $p_h$ , as previously seen, determines the concentration of active traders on the grid. For a low concentration the active traders will be distributed in small clusters and the information will be extremely split up on the grid. In this case large coherent events will be rare. A higher concentration, where clusters of the order of a thousand cells are present, allows large events to occur with higher frequency. In fact, the phase transition of large clusters can easily trigger a crash or a bubble in the market. Time series related to a higher herding parameter are therefore more intermittent. We can then infer that a market made by small groups of traders behaves like a *noisy market*, while big crashes or bubbles must necessarily be related to the interaction of large networks and so to a kind of crowd behaviour. For most of the simulations we fixed the parameter  $p_h = 0.0493$  in order to have bigger clusters, with  $S^{max}(t)$  of the order of 2500 cells.

The strength  $A$  also plays an important role in the trading dynamics. With  $p_h$  fixed, this parameter is related to the intermittency of the system. For  $A \rightarrow 0$  we observe an approach of the PDF toward a Gaussian-like shape. That is very, large fluctuations become more and more rare, and  $A$  can be regarded as a temporal scale for the system, similar to the activity parameter in the Cont-Bouchaud model [CB00]. In spite of this, some large fluctuations can be still identified. This is probably one of the main differences between the Cont-Bouchaud model and the present. In fact Monte Carlo simulations of the former [SP98] show that an increase of the activity brings a rapid convergence toward a Gaussian distribution because a large number of clusters are trading at the same time following a random procedure of decision making [CB00, SP98]: there are no clusters that can influence the market more than others and so the resulting global interaction is noise-like. In our model fluctuations are always allowed because of the heat bath dynamics. Clusters of active traders can always be subjected to phase transitions, independently of the state of other clusters, creating a displacement between demand and supply.

In order to reproduce the behaviour of financial time series we work with  $1.5 < A < 2.5$ . In this range there is a nonlinear dependence of the intermittency on  $A$ . The value of the parameter  $a$  is fixed by the relation  $a = 2A$ , already used in the work of Krawiecki et al. [KHH02]. However, we note that the ratio  $a/A$  is actually not essential in reproducing the intermittency found in real data. Even the parameter  $h$  does not have a central role in the simulation, as long as  $h \ll 1$ . In fact, the percolation dynamics of the active traders already introduces a natural noise. In most of the runs we simply set  $h = 0$ .

Now we discuss the results of the cellular automata. In Fig. 3.2 (Top) and Fig. 3.2 (Bottom) the normalized logarithmic returns of the S&P500 and of the simulation are shown, respectively. The average number of active traders, in the stable regime, is  $\approx 16000$ , as shown in Fig. 3.1 (Top). The model reproduces the intermittent behaviour of the S&P500 time series, as expressed by the *leptokurtic* PDF of Fig.3.3. The tails of the distribution follow a power law decay, reflecting the fact that large coherent events, far from the average, are likely to occur with a frequency higher than expected for a random process (where the shape would be a Gaussian). These large events are related to financial crashes or bubbles of the market and, in our model, to a phase transition in the spin state of large networks of active traders, as we will discuss further on. From a power law fit,  $P(r) \approx r^{-1-\gamma}$  (for  $|r| > 2$ ), we find  $\gamma \approx 3$  for both the S&P500 and the model, confirming the good agreement between the two.

The problem of finding the best distribution describing the price returns is a very important issue from a practical point of view [MS99]. The standard Black-Scholes theory for option pricing [BS73, MS99, PB99] assumes that the



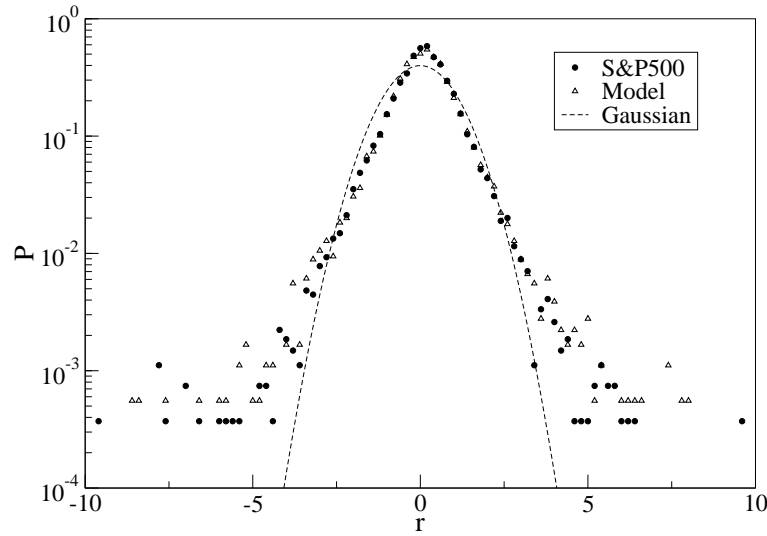


Figure 3.3: Probability distribution function for the S&P500 computed with daily data from 31/1/1950 to 18/7/2003 and the model. A Gaussian is also plotted for comparison. The parameters used are  $p_h = 0.0493$ ,  $A = 1.8$  and  $h = 0$ .

returns are normally distributed. This fact has been proven to be empirically false, as shown also in Fig. 3.3 (see Ref. [MS99] for a general reference). Finding a more appropriate distribution would be an important improvement in this field of research<sup>1</sup>.

In order to understand the trading dynamics of the automata we also show two snapshots of the grid configuration, the first during a normal session, Fig.3.4 (Top), and the second during a crash, Fig.3.4 (Bottom). During the normal session the orientations of the spins are distributed uniformly over the various clusters and there is no sharp difference between demand and supply. The situation is different during a crash. In this case the clusters at the top of the hierarchy, the bigger ones, play a fundamental role. In fact they undergo a phase transition where the greatest part of their spins share the same orientation. The capacity of the clusters to generate a coherent orientation of the spins, and hence of their trading state, can be interpreted in terms of a multiplicative noise process [PB99, Lea99], where the collective synchronization arises as a result of the randomly varying interaction strengths between agents. The peculiarity of our model is that crashes or bubbles (sudden price changes) are related not to

<sup>1</sup> An intriguing framework of investigation has been provided by the *non-extensive statistical mechanics* proposed by Tsallis [Tsa88, Tsa99, RRN<sup>+</sup>01, GC02, MJ03, AI03, TABO03].

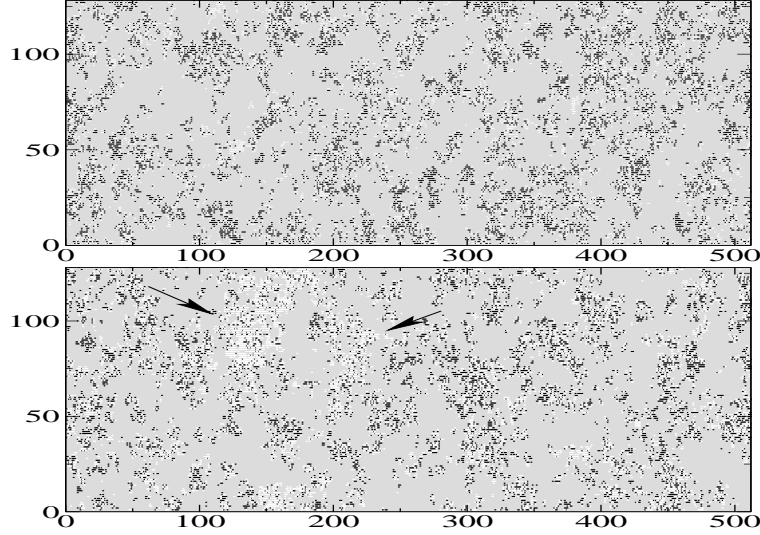


Figure 3.4: Top: snapshot of the grid during a normal trading period. The black cells are the buyers while the white ones are the sellers. The parameters used in this simulation are  $p_h = 0.0493$ ,  $A = 1.8$  and  $h = 0$ . Bottom: the same simulation during a crash. Large clusters of sellers are indicated by arrows.

a phase transition of the whole market [KHH02, Kai00] but rather to a phase transition in one or more of the larger clusters that have a greater influence on the trading session. This behaviour is probably closer to the real market where the synchronization of trading opinion is more likely to happen between large groups of traders than over the whole market.

The temporal correlations of the logarithmic returns and of the volatility are investigated via the autocorrelation function, defined as

$$\xi(\tau) = \frac{\sum_{j=1}^{L-\tau} (x_j - \bar{x})(x_{j+\tau} - \bar{x})}{\sum_{j=1}^{L-\tau} (x_j - \bar{x})^2}, \quad (3.5)$$

where  $\tau$  is a time delay and  $\bar{x}$  represents the average of the variable  $x(t) \equiv x_t$  over the period of length  $L$  under consideration. The results for both the model and the S&P500 are shown in Fig.3.5 (Top) and Fig.3.5 (Bottom), respectively. While the temporal correlation for the returns is lost almost immediately, the volatility manifests a slow decay in time, related to the phenomenon of volatility clustering. The previous temporal dependencies have been found in both real data and in the simulation.

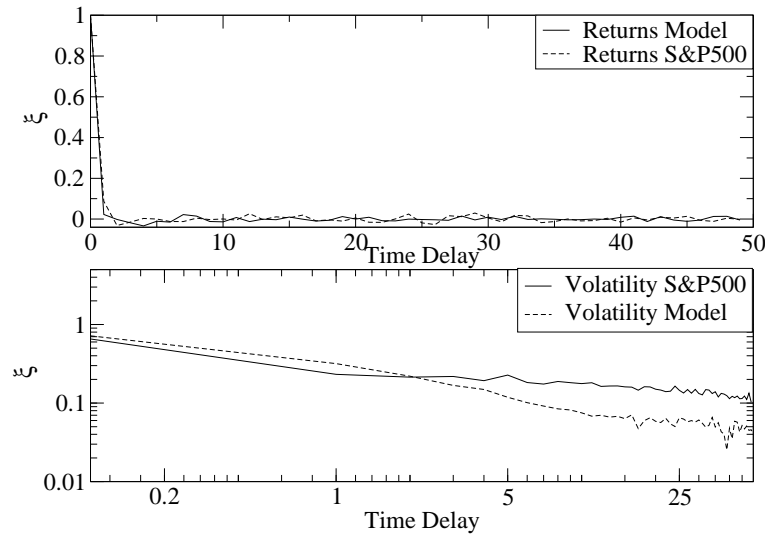


Figure 3.5: Top: Autocorrelation function for the price returns. Bottom: Autocorrelation function for the volatilities. In both the graphs the parameters used for the model are  $p_h = 0.0493$ ,  $A = 1.8$  and  $h = 0$ .

## 3.4 Multifractal analysis

It is also worth pointing out that financial time series present an inherent *multifractality* [Fed88]. In the past few years the work of many authors [RNZR<sup>+</sup>01, GDS02, AI02, DMAD03] has been addressed to the characterization of the multifractal properties of financial time series, and nowadays multifractality can be considered as a stylized fact. In order to study the multifractal properties of our model we use the *generalized Hurst exponent* [Man97],  $H(q)$ , derived via the  $q$ -order structure function,

$$S_q(\tau) = \langle |x(t + \tau) - x(t)|^q \rangle_L \propto \tau^{qH(q)}, \quad (3.6)$$

where  $x(t)$  is a stochastic variable over a time interval  $L$  and  $\tau$  the time delay. The generalized Hurst exponent, defined in (3.6), is an extension of the Hurst exponent,  $H$ , introduced in the context of reservoir control on the Nile river dam project, around 1907 [Fed88, Hur51]. This technique provides a sensitive method for revealing long-term correlations in random processes. If  $H(q) = H$  for every  $q$  the process is said to be monofractal and  $H$  is equivalent to the original definition of the Hurst exponent. This is the case of simple Brownian motion or fractional Brownian motion.

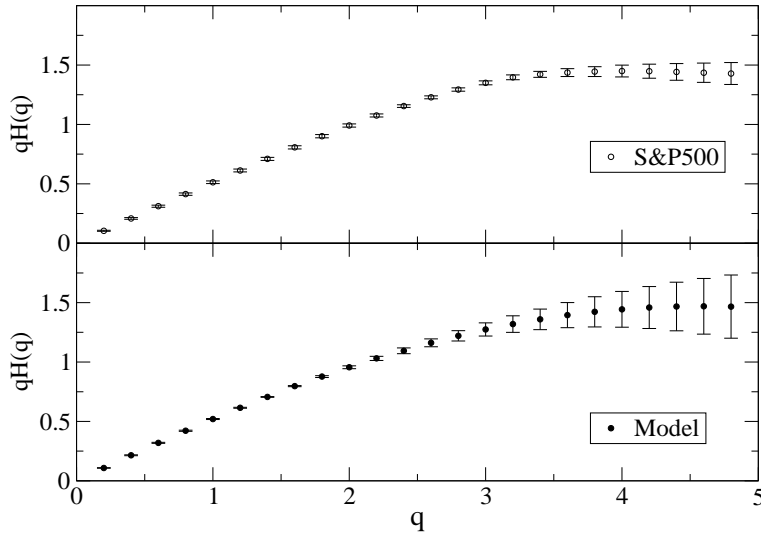


Figure 3.6: Multifractal spectra for the S&P500 in the period 31/1/1950 to 18/7/2003 (top) and the model (bottom). For the latter  $p_h = 0.0493$ ,  $A = 1.8$  and  $h = 0$ .

If the spectrum of  $H(q)$  is not constant with  $q$  the process is said to be multifractal. From the definition (3.6) it is easy to see that the function  $H(1)$  is related to the scaling properties of the volatility. By analogy with the classical Hurst analysis, a phenomenon is said to be persistent if  $H(1) > 1/2$  and antipersistent if  $H(1) < 1/2$ . For uncorrelated increments, as in Brownian motion,  $H(1) = 1/2$ . In Fig. 3.6 a comparison is shown between the multifractal spectra of the model and the S&P500 obtained from the price time series. It is clear that both processes have a multifractal structure and the price fluctuations cannot be associated with a simple random walk as in the classical *efficient market hypothesis* [Bac00].

The multifractality of the time series can also be discussed in terms of thermodynamic equivalents, according to *multifractal physics* [LH88, Can00, Can93, Vol97]. In this approach we divide the time series,  $x(t)$ , for  $t = 1, \dots, L$  into  $\mathcal{N}$  equal sub-intervals. Then we can write the following measure for each of these,

$$\mu_i(\tau) = \frac{|x(t+\tau) - x(t)|}{\sum_{t=1}^{\mathcal{N}} |x(t+\tau) - x(t)|}, \quad (3.7)$$

with  $i = 1, \dots, \mathcal{N}$  and  $\tau$  the time delay. The quantity  $\mu_i(\tau)$  can be viewed as a normalized probability measure. The corresponding generating function is given

by

$$Z(q, \tau) = \sum_{i=1}^{\mathcal{N}} \mu_i(\tau)^q \propto \mathcal{N}^{-\chi_q}, \quad (3.8)$$

that is an analogue of a generalized partition function in thermodynamics. According to Ref. [LH88] the scaling exponent  $\chi_q$  is directly related to the generalized multifractal dimension  $D_q$  [Fed88],

$$\chi_q \equiv (q - 1)D_q. \quad (3.9)$$

If we consider  $\chi_q$  as the *free energy* of our system, Eq. (3.9) provides a link between the classical thermodynamical formalism and multifractality. Assuming  $q$  as an equivalent temperature, we can define an *analogue specific heat* [LH88, Can93, Can00, ISC+02],

$$C_q = -\frac{\partial^2 \chi_q}{\partial q^2}. \quad (3.10)$$

The previous equation for  $C_q$  can also be written in terms of singular measure formalism [DMWC94]. In this framework we define a local measure in time,  $\epsilon(1, t)$ , as

$$\epsilon(1, t) = \frac{|x(t+1) - x(t)|}{\frac{1}{L-1} \sum_{t=1}^{L-1} |x(t+1) - x(t)|}. \quad (3.11)$$

We can then generate coarse-grained measures on intervals of length  $\delta$ ,  $\epsilon(\delta, l)$  where  $\delta$  is an integer power of two and  $l$  is the index of the first point of the sub segments at that resolution. The average measure in the interval  $[l, l + \delta]$  is

$$\epsilon(\delta, l) = \frac{1}{\delta} \sum_{l^*=l}^{l+\delta-1} \epsilon(1, l^*), \quad (3.12)$$

for  $l = 0, \dots, L - \delta$ . In this case we have a scaling property for the ensemble average with respect to the scale  $\delta$ :

$$\langle \epsilon(\delta, l)^q \rangle \propto \delta^{-K_q}. \quad (3.13)$$

In a multifractal process the exponent  $K_q$  is a nonlinear function of  $q$  related to the intermittency of the time series and to the generalized dimension via [HP83, HJK+86]

$$(q - 1)D_q = q - 1 - K_q. \quad (3.14)$$

From (3.10) and (3.14) we have that [ISC+02],

$$C_q = \frac{\partial^2 K_q}{\partial q^2}. \quad (3.15)$$

Following Ref. [Can00] we have found the analogue specific heat for both the S&P500 and for the price time series generated by our model, see Fig. 3.7. For  $\tau = 1$  we observe a double-humped shape for both the model and the empirical data. If we take longer time delays the shoulder on the right hand side disappears, leaving only a sharp peak, similar to a first order phase transition around  $q = -1.5$ . The results are in agreement with the analysis of Canessa [Can00] and recall the Hubbard model for small to intermediate values of the local interaction [Vol97]. As also suggested in Ref. [Can00], the second peak is due to the large fluctuations at small scales, that is crashes and bubbles. Increasing the time delay means that the fluctuations tend to be smoothed and the time series of returns approach a noise-like regime. For this reason the analogue specific heat shapes for  $\tau = 100$  are basically indistinguishable. From this argument we can interpret the analogue specific heat, and in particular the second peak for low time delays, as a way to characterize crashes, or in general the degree of intermittency in a time series. The difference in the shapes and heights of the shorter peak for  $\tau = 1$  is due to a slightly different correlation of the fluctuations in the two time series. Moreover, in the model we can link the shorter peak to the physical phase transition in the spin state of a network of traders.

## 3.5 Discussion and conclusion

In the present chapter, in order to mimic the dynamics of the financial markets, we have introduced a stochastic cellular automata model. The main difference between our model and other stochastic simulations based on spin orientation of agents [KHH02, Kai00] is the temporal evolution of the networks of interaction and therefore the concept of an “open” market. The active traders follow a direct percolation dynamics in order to aggregate in networks of information. This makes our simulation, even if still a raw approximation, surely closer to the real market, where no conservation rules for the number of agents can be claimed. Crashes and bubbles can be interpreted as a synchronization of the spin orientation of the more influential networks in the market. The model is able to reproduce most of the stylized aspects of the financial time series, supporting the idea that crashes and bubbles are related to a collective synchronization in the trading behaviour of large networks of traders, where the information is exchanged according stochastic interaction between them.

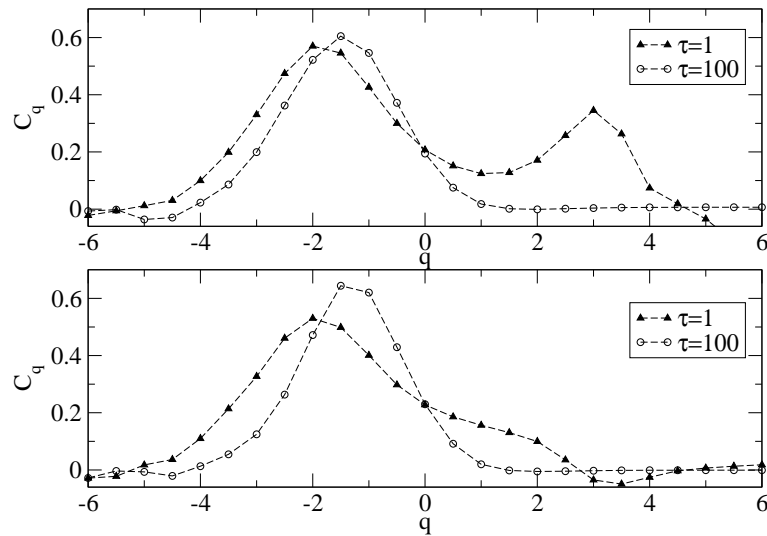


Figure 3.7: Top: analogue specific heat for the S&P500 from 31/1/1950 to 18/7/2003 for two different time delays, namely  $\tau = 1$  and  $\tau = 100$ . A sharp peak is clearly visible around  $q = -1.5$ . The second peak on the right hand side disappears increasing the temporal delay. The  $C_q$  curves have been computed for the logarithm of the price using the algorithm in [DMWC94] for  $K_q$ . Bottom: analogue specific heat for the model with parameters  $p_h = 0.0493$ ,  $A = 1.8$  and  $h = 0$ . The double humped shaped for small temporal delays is visible also here.